

SPARTICLE RECONSTRUCTION AT LHC

ALESSIA TRICOMI

on behalf of the ATLAS and CMS Collaborations

*Department of Physics and Astronomy, University of Catania, and INFN Catania,
Via S. Sofia 64, I-95123 Catania, Italy*

In this report a review of recent studies made to understand the capability to discover and measure properties of SUSY particles at LHC is discussed. The expected resolution on sparticle masses is discussed on the basis of studies performed by the ATLAS and CMS collaborations.

1 Introduction

One of the main purposes of the LHC collider is to search for Physics beyond the Standard Model (SM). Supersymmetric (SUSY) extensions of SM¹ predict the existence of superpartners for all ordinary particles. If supersymmetry exists at the electroweak scale, it could hardly escape detection at LHC. The centre-of-mass energy of 14 TeV, available at LHC, extends the searches for SUSY particles up to masses of 2.5 to 3 TeV/ c^2 . In R-parity conserving models, the stable Lightest Supersymmetric Particles (LSP), which escape detection, lead to events characterized by large missing energy. Usually, squarks and/or gluinos are the most abundant sparticles produced at LHC. They decay in a number of steps to quarks, charginos, neutralinos, sleptons, W, Z, Higgs bosons, etc. These events are expected to show up at LHC via an excess of multijet+ E_T^{miss} +multilepton final states compared to the SM expectations².

A significant part of the efforts in preparation for the LHC startup is being spent in the simulations of the new physics potential. In the past years, the simulation studies have been mainly devoted to understand the discovery reach of SUSY particles through inclusive studies. In these studies, the typical discovery strategy consists in searching for an excess of events with a given topology with respect to the Standard Model expectations. A variety of final state signatures has been considered. Inclusive studies have mainly been carried out in the framework of mSUGRA^{3,4}, with five independent parameters: the common gaugino mass $m_{1/2}$, the common scalar mass m_0 , the common trilinear scalar coupling A_0 , the ratio of the vacuum expectation values of the two Higgs doublets $\tan\beta$ and the sign of the Higgsino mixing parameter μ . Strong

indications exist, however, that the overall SUSY reach in terms of masses of squarks and gluinos is very similar in most the R-parity conserving scenarios, provided that $m_{\chi_1^0} \ll m_{\tilde{g}, \tilde{q}}$. This has been shown to be the case for the AMSB model⁵ and even for the MSSM⁶. Already with only 1 fb^{-1} of integrated luminosity, LHC should be able to discover squarks and gluinos if their masses do not exceed about $1.3 \text{ TeV}/c^2$. With 100 fb^{-1} the reach can be extended up to masses $m_{\tilde{q}} \sim m_{\tilde{g}} \sim 2.5 \text{ TeV}/c^2$. The entire plausible domain of EW-SUSY parameter space for most probable value of $\tan\beta$ can be probed.

Determining the masses of supersymmetric particles is more difficult, because each SUSY event contains two LSP's, and there are not enough kinematic constraints to determine the momenta of these particles. The main goal of this report, is to show the potential of the ATLAS⁷ and CMS detectors⁸ to reconstruct SUSY particles and the achievable mass resolution.

2 SUSY Particle Measurements

The reconstruction of sparticle masses and the determination of their properties might help in probing different models. In order to reconstruct sparticle masses, a different strategy with respect to that developed for inclusive analyses must be used. The typical procedure consists of several steps: (i) choose a set of benchmark points compatible with all existing measurements and spanning the whole SUSY parameter space, (ii) choose a particular decay chain, (iii) get the mass spectrum, exploit the kinematical properties such as the presence of characteristic end points or thresholds, and finally (iv) try to reconstruct sparticles using constraints from various mass combinations⁹.

The choice of benchmark points depends on the purpose of the actual investigation. A large variety of benchmark points have been proposed in the past. The studies presented in this report rely on a set of points^{4,10,11}, which takes into account constraints from LEP results, cosmology measurements and low-energy experiments.

2.1 Dilepton edge reconstruction

Squark and gluino decays are often characterized by long decay chains in which the next-to-lightest neutralino (χ_2^0) is abundantly produced. The χ_2^0 may then decay into the LSP through the chain $\chi_2^0 \rightarrow \tilde{\ell}^\pm \ell^\mp \rightarrow \chi_1^0 \ell^+ \ell^-$. Leptons (electrons and muons) from the χ_2^0 decay exhibit a $\ell^+ \ell^-$ invariant mass distribution with a sharp edge. If $m_{\chi_2^0} < m_{\tilde{\ell}} + m_\ell$, the χ_2^0 decay is a three body decay mediated by a virtual slepton and the edge is placed at $m_{\chi_2^0} - m_{\chi_1^0}$. Similarly, when $m_{\chi_2^0} > m_{\tilde{\ell}} + m_\ell$, the neutralino decay is a two-body decay and the corresponding edge is placed at

$$M_{\ell^+ \ell^-} = \frac{\sqrt{(m_{\chi_2^0}^2 - m_\ell^2)(m_{\tilde{\ell}}^2 - m_{\chi_1^0}^2)}}{m_{\tilde{\ell}}}. \quad (1)$$

Figure 1 shows the same-flavour opposite-sign (SFOS) dilepton invariant mass distribution for a CMS simulation probing the point B of Ref.¹⁰. The Standard Model background, due mostly to $t\bar{t}$ and Z +jet events (Fig. 1a), is rejected by a cut on the transverse missing energy. The remaining contribution is clearly negligible. The real background comes from other SUSY processes, and, as is illustrated in Fig. 1b, is effectively removed by subtracting the contribution of opposite-sign opposite-flavour dilepton pair (OSOF) distribution. The edge value for $M_{\ell^+ \ell^-}$ is determined by fitting it to a triangular shape with Gaussian smearing.

For large values of $\tan\beta$, the χ_2^0 decays predominantly to $\tilde{\tau}$'s (and therefore τ 's). In this configuration, it is more difficult to clearly identify the dilepton edge. It is hoped that hadronic τ decays, with appropriate cuts and selections could still lead to an end point in the $\tau\tau$ mass distribution, as is shown in Ref.^{4,12} for the ATLAS Point 6 or for point SPS1A.

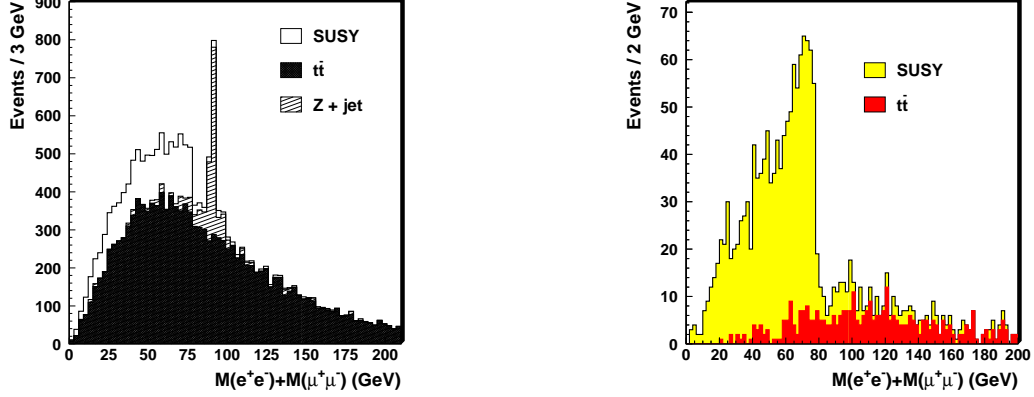


Figure 1: (a) Invariant mass distribution of SFOS isolated leptons for \tilde{q} and \tilde{g} events, superimposed on the SM background. The contributions of $t\bar{t}$ and Z+jets events are shown. (b) Same as in (a) with $E_T^{\text{miss}} > 150$ GeV cut.

2.2 Squark and Gluino Mass Reconstruction

The reconstruction of a χ_2^0 is the starting point for more complex decay chain reconstruction. Here, the technique used by CMS for squarks and gluino mass determination is briefly summarized. Three out of the thirteen “Post-LEP” benchmark points have been used for this analysis, the point B ($m_{1/2} = 250$ GeV/ c^2 , $m_0 = 100$ GeV/ c^2 , $\tan\beta = 10$, $\mu > 0$ and $A_0 = 0$), G ($m_{1/2} = 375$ GeV/ c^2 , $m_0 = 120$ GeV/ c^2 , $\tan\beta = 20$, $\mu > 0$ and $A_0 = 0$) and I ($m_{1/2} = 350$ GeV/ c^2 , $m_0 = 180$ GeV/ c^2 , $\tan\beta = 35$, $\mu > 0$ and $A_0 = 0$) of Ref. ¹⁰, characterized both by relatively low value for m_0 and $m_{1/2}$ (high \tilde{q} and \tilde{g} production cross section) and different values of $\tan\beta$. In order to perform $\tilde{b}(\tilde{q})$ and \tilde{g} mass reconstruction, the decay chain $\tilde{g} \rightarrow \tilde{b}b$, $\tilde{b} \rightarrow \chi_2^0 b$, $\chi_2^0 \rightarrow \tilde{\ell}^\pm \ell^\mp \rightarrow \chi_1^0 \ell^+ \ell^-$, where $\ell = e, \mu$, have been considered. The same decay chain with light quark replacing sbottom has been used for squark reconstruction. The events are selected by requiring at least two SFOS isolated leptons with $p_T > 15$ GeV/ c and $|\eta| < 2.4$, corresponding to the acceptance of the muon system, and two jets (tagged as b jets in the case of sbottom reconstruction), with $p_T > 20$ GeV/ c and $|\eta| < 2.4$. A cut on the missing energy is applied in order to suppress the SM background. The first step of the reconstruction proceeds as described in the previous paragraph from the dilepton edge. To reconstruct the sbottom (squark), events in a window about 15 GeV/ c^2 wide around the edge are selected. This requirement allows the kinematical configuration in which the leptons are emitted back-to-back in the χ_2^0 rest frame, with the χ_1^0 at rest, to be selected. In this configuration the χ_2^0 momentum is reconstructed through the relation

$$\vec{p}_{\chi_2^0} = \left(1 + \frac{m_{\chi_1^0}}{M_{\ell^+\ell^-}}\right) \vec{p}_{\ell^+\ell^-}. \quad (2)$$

Here, the χ_1^0 mass is assumed to be known. A method to extract the χ_1^0 mass from the data is discussed in the next section. The χ_2^0 momentum is then added to the momentum of the highest E_T (b-tagged) jet. The \tilde{q} (\tilde{b}) is reconstructed, as shown in Figs. 2a and 2b. To reduce the combinatorial background coming from wrong (b) jet associations, further kinematical cuts are used. The reconstruction of squarks in a scenario similar to point B is feasible already with an integrated luminosity of 1 fb⁻¹, while in the case of the sbottom at least 10 fb⁻¹ are necessary to achieve a mass resolution better than 10%. Finally, the squark (sbottom) associated with the closest (b) jet in space gives the reconstructed gluino mass, as shown in Fig. 2c. A resolution better than 10% is achieved also in this case. To summarize, in the case of a precise knowledge of the χ_1^0 mass, the mass resolution achievable for each of the sparticles considered is about 10%

for 10 fb^{-1} . The dependence of the reconstructed masses on the χ_1^0 mass uncertainty has been evaluated in Ref. ¹³ to be

$$\Delta m(\chi_2^0 b) = (1.60 \pm 0.03) \Delta m(\chi_1^0). \quad (3)$$

Although both $m(\tilde{q})$ and $m(\tilde{g})$ depend on the χ_1^0 mass, their difference is in contrast independent of $m(\chi_1^0)$ and can be measured with an error of few percent, irrespective of the sparticle spectrum ¹³.

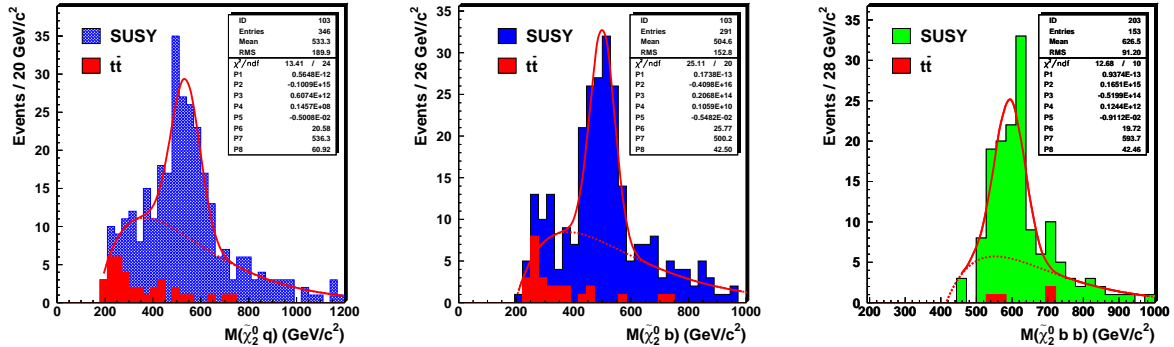


Figure 2: Reconstructed invariant mass distribution for squark (left), sbottom (middle) and gluino in the sbottom chain (right) at point B. The integrated luminosity is 1 fb^{-1} for the squark peak and 10 fb^{-1} for the sbottom and the gluino peaks.

All the results shown so far are derived for point B (with parameters similar to that of point SPS1A) and for an integrated luminosity of 10 fb^{-1} . The same kind of analysis was repeated also for point G. In this case, however, the higher value of $\tan \beta$ reflects into higher branching ratio for the decay $\chi_2^0 \rightarrow \tau^+ \tau^- \chi_1^0$, hence to a smaller signal $\chi_2^0 \rightarrow \tilde{\ell}^\pm \ell^\mp \rightarrow \chi_1^0 \ell^+ \ell^-$, $\ell = e, \mu$. Reconstruction of squarks and gluinos is only possible with tighter cuts and with high integrated luminosity. An attempt was made to repeat the analysis at point I of Ref. ¹⁰, characterized by a yet higher value of $\tan \beta$ ($\tan \beta = 35$). For that point, even with an integrated luminosity of 300 fb^{-1} , it is not possible to reconstruct squarks and gluinos with this method.

2.3 χ_1^0 Mass Determination

In sequential decays, the presence of other end points and thresholds, as suggested in Ref. ⁹, can be used to extract, in a model-independent way, the masses of the sparticles, and, finally, to disentangle different models. The starting point is the same decay chain as in the previous section. The two leading jets are assumed to come from the squark decays and are combined with the lepton to find other end points and thresholds. For example, the largest dilepton-jet mass, $M_{\ell\ell q}$ and the largest lepton-jet masses, for the first and the second lepton, $M_{\ell q}^{\max}$ and $M_{\ell q}^{\min}$, are expected to give end points as well as $M_{\ell\ell q}$ should give a threshold. The distributions of these quantities are shown in Fig. 3. Other end points are clearly visible and well measurable, despite various detection and reconstruction spoiling factors. With the high statistics reachable at LHC, it seems possible to measure the end points with a precision limited only by the hadronic scale accuracy (1 to 2% depending on the particle combinations for point B or SPS1A).

It is possible to extract the masses of the sparticles with a combination of all these end point measurements. In particular, the mass of χ_1^0 is a fundamental ingredient of the other sparticle mass measurements. In Fig. 4, the reconstructed χ_1^0 mass peak is shown. A resolution of about 10% is achievable, within a given model.

In Fig. 5 the result of the fits with the mSUGRA Point 5 (S5) and the point in an Optimized String Model (O1) ⁹ are compared.

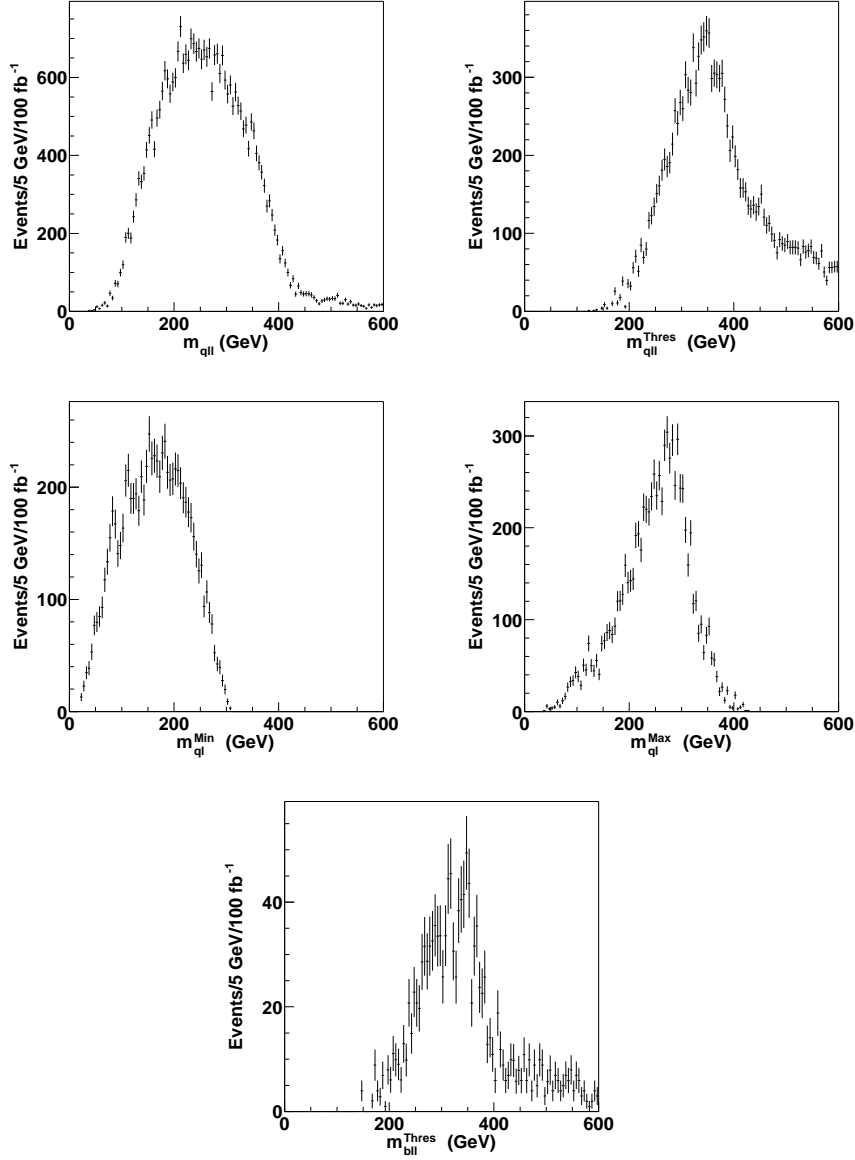


Figure 3: ATLAS invariant mass distributions with kinematical end points for the mSUGRA Point SPS1A.

Conclusions

If SUSY exists at the EW scale, both the ATLAS and CMS will be able to discover it over a large range of the parameter space. Squark and gluino decays present characteristic signatures to discriminate the SUSY processes from the Standard Model. Inclusive studies have demonstrated that squarks and gluinos could be discovered already in the first months of data taking. With the ultimate luminosity of 300 fb^{-1} , strongly interacting sparticles could be discovered up to masses of 2.5 to 3 TeV/c^2 .

Although sparticle reconstruction is more difficult, new analyses have shown that in some cases it is possible to make exclusive reconstructions. A search for special features, like kinematical end points and thresholds, excesses of b/τ 's, isolated leptons helps in the reconstruction of full decay chains and, possibly, to disentangle different theoretical models. This is the case, for instance, for the decay $\tilde{g} \rightarrow \tilde{q}(\tilde{b})q(b)$ which allows both squark (sbottom) and gluino masses to

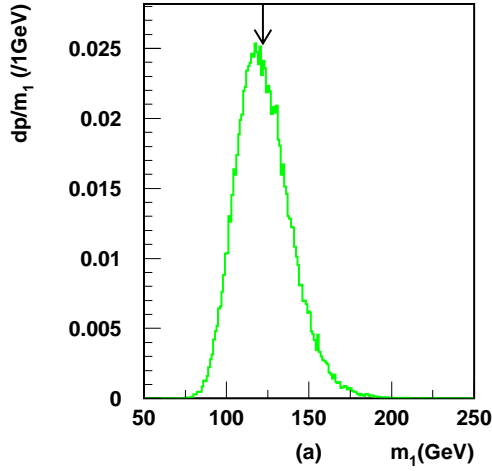


Figure 4: $M(\chi_1^0)$ distribution for ATLAS point 5.

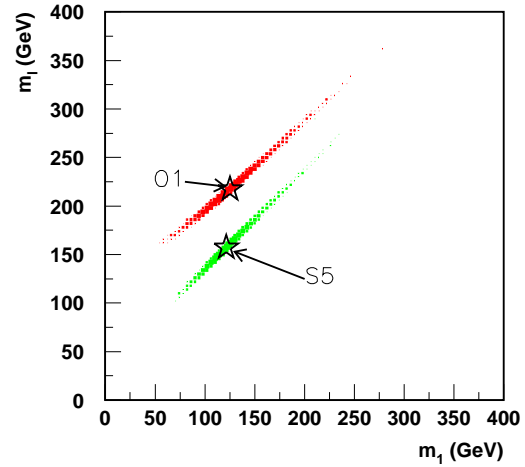


Figure 5: Reconstructed $M(\tilde{\ell})$ vs $M(\chi_1^0)$ for O1 and S5 (see text). The stars show the true mass for each model.

be reconstructed. Resolutions better than 10% are attainable in the low $\tan\beta$ region, already after the first year of data taking. More work is in progress to evaluate the ATLAS and CMS capability to reconstruct SUSY sparticles.

Acknowledgments

I would like to thank the Conference Organizers for the invitation and for the friendly hospitality. Special thanks also to M. Chiorboli and G. Polesello for providing materials for the presentation and helpful discussion. I would like also to thank P. Janot for the reviewing.

References

1. H.P. Nilles, *Phys. Rev.* **110**, 1 (1984)
2. H. Baer, C.H. Chen, F. Paige and X. Tata, *Phys. Rev. D* **52**, 2746 (1995); *Phys. Rev. D* **53**, 6241 (1996).
3. S. Abdullin and F. Charles, *Nucl. Phys. B* **547**, 60 (1999); S. Abdullin, Ž. Antunović and M. Dželalija, *Mod. Phys. Lett. A* **15**, 465 (2000).
4. The ATLAS Collaboration, *ATLAS Detector and Physics Performance Technical Design Report*, CERN/LHCC 99-014 (1999).
5. A.J. Barr *et al.*, *JHEP* **0303** (2003) 045.
6. S. Abdullin, A. Albert and F. Charles, in *Proceedings of Les Houches 2001, Physics at TeV colliders*, p. 161, ed. P. Aurenche *et al.*, (Paris, IN2P3, 2001).
7. The ATLAS Collaboration, Technical Proposal, CERN/LHCC 94-043 (1994).
8. The CMS Collaboration, CERN/LHCC 94-038 (1994).
9. B.C. Allanach *et al.*, *JHEP* **0009** (2000) 004.
10. M. Battaglia *et al.*, *Eur. Phys. J. C* **22** (2001) 535.
11. B.C. Allanach *et al.*, hep-ph/0202233 (2002).
12. B.K. Gjelsten *et al.* ATLAS-PHYS-2004-007 (2004).
13. M. Chiorboli and A. Tricomi, *Squark and Gluino Reconstruction with the CMS Detector*, CMS RN-2003/002 (2003).